HHS Public Access

Author manuscript

Heart Rhythm. Author manuscript; available in PMC 2021 April 08.

Published in final edited form as:

Heart Rhythm. 2021 April ; 18(4): 579–588. doi:10.1016/j.hrthm.2020.12.003.

Prognostic value of cardiac magnetic resonance septal late gadolinium enhancement patterns for periaortic ventricular tachycardia ablation: Heterogeneity of the anteroseptal substrate in nonischemic cardiomyopathy

Takuro Nishimura, MD, PhD[*], **Hena N. Patel, MD**[†], **Shuo Wang, MD**[†], **Gaurav A. Upadhyay, MD, FHRS**[*], **Heather L. Smith, MD, PhD**[‡], **Cevher Ozcan, MD**[*], **Dalise Y. Shatz, BA**[*], **Hemal M. Nayak, MD, FHRS**[*], **Amit R. Patel, MD**[†], **Roderick Tung, MD, FHRS**[*]

[*] Center for Arrhythmia Care, University of Chicago Medicine, Pritzker School of Medicine, Chicago, Illinois

[†] Cardiac Imaging Center, University of Chicago Medicine, Pritzker School of Medicine, Chicago, Illinois

[‡] Department of Pathology, University of Chicago Medicine, Pritzker School of Medicine, Chicago, Illinois.

Abstract

BACKGROUND—Ventricular tachycardia (VT) from the anteroseptal subtype of nonischemic cardiomyopathy has a high probability of recurrence after catheter ablation.

OBJECTIVE—The purpose of this study was to determine the predictive value of septal scar patterns by late gadolinium enhancement (LGE) cardiac magnetic resonance (CMR) on ablation outcomes in patients with VT arising from an anteroseptal substrate.

METHODS—Patients with periaortic VT arising from an anteroseptal substrate with preprocedural wideband LGE-CMR were divided into 2 groups by the degree of longitudinal septal LGE extension as full-length septal (≥80% anteroposterior length) or partial septal (<80% anteroposterior length). Septal LGE volumes were quantified in those with and without VT recurrence.

RESULTS—Among 234 patients referred for scar-related VT ablation between 2017 and 2020, 25 patients (92% male; age 64 ± 8 years) and a total of 108 VTs were analyzed. A greater number of VT morphologies were induced in patients with full-length septal LGE compared to partial septal LGE (median [interquartile range]: 5 [3–9] vs 2 [1–4]; $P = .005$). Patients with VT recurrence had larger septal LGE volumes compared to those without recurrence (11.4 mL [8.8–13.9] vs 4.2 mL [0–9.5]; $P = .012$). At median follow-up of 16 months (5–22), overall freedom

Address reprint requests and correspondence: Dr Roderick Tung, The University of Chicago Medicine, 5841 S. Maryland Avenue, MC 6080, Chicago, IL 60637. rodericktung@uchicago.edu.

Appendix

Supplementary data

Supplementary data associated with this article can be found in the online version at https://doi.org/10.1016/j.hrthm.2020.12.003.

from VT recurrence was 52% and significantly higher in patients with partial septal LGE than in those with full-length septal LGE (80% vs 20%; $P = .005$).

CONCLUSION—VT originating from an anteroseptal substrate is associated with heterogeneous patterns and extent of CMR septal scar. Preprocedural imaging may substratify this challenging patient population for the propensity for multiple induced VT morphologies and recurrence after catheter ablation.

Graphical Abstract

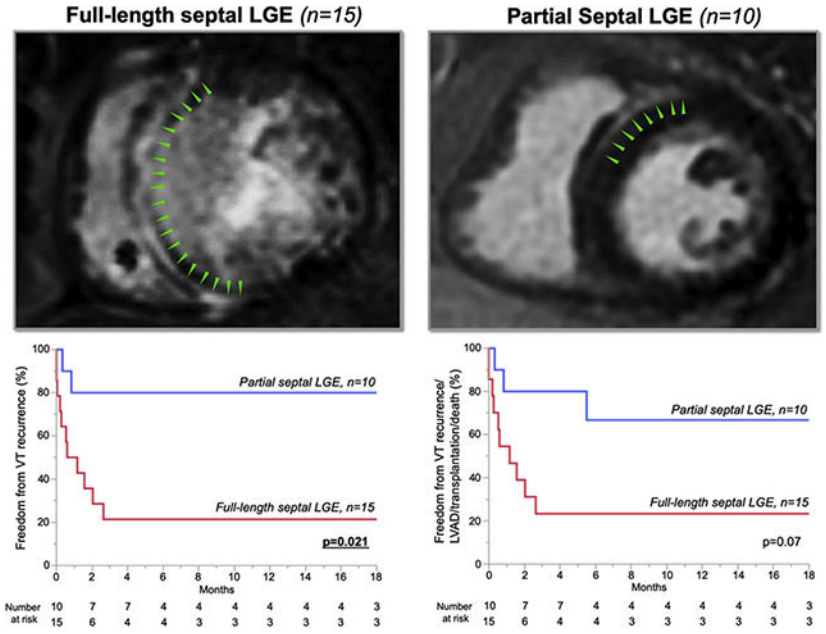

Keywords

Ablation; Cardiac magnetic resonance; Magnetic resonance imaging; Late gadolinium; Septal scar; Ventricular tachycardia

Introduction

The interventricular septum is a challenging substrate location for scar-related ventricular tachycardia (VT), often causing multiple VT morphologies and often refractory to standard radiofrequency (RF) ablation.[1,2] Among patients with nonischemic cardiomyopathy (NICM), anteroseptal subtypes are associated with higher rates of recurrence (50%–74%) after catheter ablation compared to inferolateral substrates.[3,4] Late gadolinium enhancement (LGE) cardiac magnetic resonance (CMR) imaging has been shown to be predictive of arrhythmogenic risk in patients with structural heart disease[5,6] and identifies potential targets sites for catheter ablation.[7] The prognostic value of the extent and pattern of septal involvement for ablation outcomes has not been analyzed within this increasingly referred population with anteroseptal substrate. We hypothesized that the patterns of septal scar detected by LGE-CMR can predict the spectrum of induced VT morphologies and subsequent risk for VT recurrence after catheter ablation.

The aims of the present study were to describe the spectrum of VT morphologies and successful ablation sites associated with septal LGE patterns and to investigate the prognostic value of the pattern and extent of septal LGE in patients with scar-related anteroseptal VT.

Methods

Consecutive patients were identified if they showed evidence of periaortic VTs with anteroseptal substrate by preprocedural CMR and/or electroanatomic mapping from March 2017 to September 2020. Patients were enrolled from a prospective University of Chicago VT Ablation Registry (IRB16–0272) and retrospectively analyzed. Periaortic VT was defined as VT with a critical site within 2 cm from the ventriculo-aortic junction as previously described.[8] Review of these data was approved by the institutional review board at University of Chicago Medical Center. The research adhered to the Declaration of Helsinki as revised in 2013.

CMR imaging protocol

CMR imaging was performed using a 1.5-T scanner (Achieva, Philips Medical Systems, Andover, MA) with a 5-channel surface coil. Retrospectively gated short-axis cine images were obtained spanning the left ventricle (LV) from base to apex and also in the 2-, 3-, and 4-chamber views. LGE acquisition and quantification are described in the Supplemental Methods. In brief, 10 minutes after administration of gadolinium, LGE images were acquired in the same views using a T1-weighted gradient-echo pulse sequence (typical inversion time [TI] 200–300 ms set per T1 Look–Locker scout, voxel size 2 × 2 × 10 mm, sensitivity encoding factor 2). Phase sensitive inversion recovery reconstruction was used. In patients with an implantable cardioverter-defibrillator, a wideband version of the LGE technique was utilized.[9]

Assessment of LGE involvement in anteroseptal region

The presence of LGE was interpreted and quantified by 2 independent observers trained in advanced imaging (HP, SW), blinded to procedural and clinical outcomes. LGE was defined as having a signal intensity >5 SD of the normal remote myocardium and seen either on 2 contiguous slices or in 2 different imaging planes (Supplemental Methods). Oblique images were used to confirm that an area of suspected LGE was not due to partial volume effect from the LV outflow tract.

Patients were divided into 2 groups based on the extent of septal longitudinal LGE involvement, defined as the region between the anterior and inferoposterior right ventricular (RV) insertion points (Figures 1A and 1B):

1. *Full-length septal LGE (FS)* consisted of patients with ≥80% anteroposterior length of LGE involvement of interventricular septum.
2. *Partial septal LGE (PS)* consisted of patients with <80% anteroposterior length of LGE involvement. For grouping, the LGE percentage was quantified from the short-axis slice that revealed the largest extent of septal LGE.

The degree of LGE extension along the long axis of the interventricular septum and whether it involved the epicardial, midwall, or endocardial layer were determined. The total volume of LGE and the percentage of LGE relative to the volume of the septal myocardium were calculated using the method of disks.

We further defined 2 morphologic patterns of concomitant LGE with anteroseptal LGE (Figure 2A):

1. *RV extension (T-shaped pattern)*: In addition to LV anteroseptal region, LGE is observed in the adjacent right ventricular outflow tract (RVOT).
2. *LV extension (C-shaped pattern)*: LGE continuously extends from ventricular septum into the LV anterior and inferior walls beyond the RV insertion points.

Voltage mapping during baseline rhythm

High-resolution mapping was performed using the EnSite system (Precision, Abbott, Abbott Park, IL) with a duodecapolar linear catheter (Livewire, Abbott) or grid catheter (HD Grid Advisor, Abbott). In voltage analysis, low voltage was defined as a peak-to-peak bipolar electrogram amplitude <1.5 mV and <8.3 mV for bipolar and unipolar, respectively, in the LV septum (Figure 3A).[10,11]

VT induction and ablation

After electroanatomic mapping during baseline rhythm, programmed stimulation was performed in areas with abnormal substrate (fractionation, split, or late potentials) with basic drive of 400 ms and up to triple extrastimuli.

RF ablation was performed using an open-irrigated catheter (FlexAbility SE, Abbott) at 30–50 W with temperature limit of 45°C. Ablation was performed until local electrograms were reduced or eliminated within deceleration zones.[12]

Follow-up

Patients underwent routine clinical follow-up in the outpatient clinic setting with device interrogation within the first month of ablation and every 3–6 months thereafter. The primary endpoint was VT recurrence. Secondary endpoints included freedom from the composite of VT, left ventricular assist device (LVAD) implantation, heart transplantation, or death. VT recurrence was defined as sustained monomorphic VT >30 seconds or any appropriate device therapy with antitachycardia pacing or shock.

Statistical analysis

Continuous variables are expressed as mean ± SD if normally distributed or median (interquartile range) if not normally distributed. Categorical variables are expressed as number (percentage) and were compared using the χ^2 test of association or Fisher exact test. The sensitivity and specificity of the length of septal LGE involvement to categorize FS and PS was assessed by constructing receiver operating characteristic curve analysis (Supplemental Methods and Supplemental Figure 1). Interclass correlation coefficients were used to determine the inter- and intraobserver variability for determining the area of LGE in

the septum, and T-shaped and C-shaped pattern. A paired Student *t* test or Wilcoxon rank-sum test (Mann-Whitney) was used to estimate differences between 2 groups. Two-sided probability level $P < .05$ was considered significant. Kaplan-Meier time-to-event analysis was generated to describe time to VT recurrence, tested with log-rank tests. Analyses were conducted using JMP Version 12.2.0 (SAS Institute, Cary, NC).

Results

Baseline characteristics

Among 234 patients who underwent scar related VT ablation, 33 patients (14%) with anteroseptal substrate underwent ablation to target periaortic VT between March 2017 and September 2020. Preprocedural CMR was performed in 25 patients (92% male; age 64 ± 8 years) to characterize scar substrate. Baseline patient characteristics are listed in Table 1. All but 1 patient had a pre-existing implantable cardioverter-defibrillator and underwent wideband CMR sequences to mitigate device-related artifact. FS was observed in 15 patients and PS in 10 patients by CMR. Four patients had mixed cardiomyopathy with concomitant history of coronary artery disease (FS 1, PS 3) (Supplemental Figure 2). Lamin A/C cardiomyopathy was confirmed by genetic testing in 3 patients (FS 2, PS 1).

Median ejection fraction was 39% (24%–47%), which was numerically but not significantly lower in patients with FS compared to PS (30% [22%–45%] vs 43% [35%–51%]; $P = .19$). VT storm was present in 32% of cases (n = 8), and 80% (n = 20) had not responded to amiodarone. Fifty-three percent (n = 8) and 40% (n = 4) of patients with FS and PS, respectively, had undergone previous VT ablation ($P = .69$).

LGE-CMR analysis

LGE imaging with wideband yielded interpretable images in all patients, although the RVOT was obscured by device artifact in 3 patients. Among all patients, septal LGE involved 82% (53%–100%) of the entire anteroposterior length, with 100% (74%–100%) of the length involved in FS and 43% (0%–72%) of length involved in PS. LGE involving the septal midmyocardial layer was observed in 76% of patients (n = 19). Overall septal LGE volume was 9.2 mL (3.8–12), which was larger in patients with FS than PS (9.8 mL [8.9–13.5] vs 3 mL [0–8.5]; $P = .009$) (Figure 1C). Septal LGE volume was not significantly different between patients with and without previous VT ablation (9.2 mL [5.4–13.9] vs 9.1 mL [0–11.5]; $P = .36$.) Among patients with PS, septal substrate was evident by electroanatomic mapping in only 3 without septal LGE (Supplemental Figure 3).

RV extension (T-shaped pattern) was observed in 24% of patients (n = 6). Twenty percent of FS patients (n = 3) and 30% (n = 3) of PS patients had a T-shaped pattern. LV extension (C-shaped pattern) was observed in 32% of patients (n = 8) (Figure 2B). All C-shaped LGE was observed in the basal LV (basal third of the long axis), and 75% (n = 6) extended to the middle portion.

There was significant agreement between observers with inter- and intraobserver variability for detecting the LGE area in septum, and C-shaped and T-shaped pattern (interclass correlation coefficient 0.93–0.99) (Supplemental Table 1).

Comparison of voltage mapping and CMR

Voltage maps during baseline rhythm were created with 2325 ± 1400 points. Median unipolar abnormal voltage area in the septum was 44 cm^2 (26–68), and bipolar voltage abnormal area was 29 cm^2 (15–42). Between those with FS and PS, the septal low-voltage area was larger in both unipolar voltage analysis (57 cm^2 [40–71] vs 27 cm^2 [16–44]; *P* = .012) and bipolar voltage analysis (37 cm^2 [21–45] vs 17 cm^2 [11–36]; *P* = .07), respectively. Abnormal voltage area was recorded in all 3 patients without LGE, in whom unipolar and bipolar low-voltage area was 15 cm^2 (9–54) and 10 cm^2 (6–44), respectively. Unipolar abnormal voltage area correlated with LGE volume (r = 0.68; *P* = .002), whereas bipolar abnormal voltage area did not show correlation with septal LGE volume (r = 0.31; *P* = .21) (Figure 3).

VT characteristics based on LGE involvement

A total of 108 VTs were induced, of which 37% (n = 40) originated from within the periaortic region. Median cycle length was 381 ms (310–440). VT morphology distribution is given in the Supplemental Results. A greater number of distinct VT morphologies were induced in those with FS compared to PS (5 [3–9] vs 2 [1–4]; *P* = .005) (Figure 4). The number of VT morphologies was larger in patients with midmyocardial layer involvement compared to those without (5 [3–7] vs 2 [1–2]; *P* = .001). The number of morphologies of VT was the greatest in those with C-shaped septal scar patterns compared to those without (6 [3–10] vs 3 [2–5]; *P* = .027). VTs with superior axis were more frequently induced in patients with FS compared to those with PS (60% vs 10%; *P* = .018). Morphologies consistent with exit from the RVOT (left bundle branch block pattern VT with late transition [$>V_3$])[13] were equally induced in patients with T-shaped pattern compared to those without (50% vs 53%; *P* = 1).

Ablation and acute outcome

Thirty-five percent of induced VTs (n = 38) were acutely terminated by RF ablation, of which 68% (n = 26) had critical sites within the anteroseptal region. A median of 3 (1–5) RF applications were delivered to terminate VT with a median time to VT termination during RF energy delivery of 9 seconds (4–33). VT termination in patients with septal midmyocardial involvement required longer RF application compared to VTs in patients without (17 seconds [6–34] vs 2 seconds [2–3]; *P* = .005). Total RF time in the procedure was longer for patients with FS compared PS (36 ± 20 minutes vs 18 ± 9 minutes; *P* = .019). Bipolar ablation was performed in 3 patients, among whom 2 had a C-shaped pattern.

VT termination sites correlated with the area of LGE involvement (Supplemental Figure 4). Three VTs were terminated from the RVOT in 2 patients with T-shaped pattern. Two VTs were terminated from the RV parahisian region, with 1 VT also terminated from the LV with a longer RF application (Figure 5).

Achievement of non inducibility of any VT was observed in 60% of FS (n = 9) and 90% of PS patients (n = 9) (*P* = .086). Median procedural time was 5.1 hours (3.6–6.9), with FS patients requiring significantly longer procedures compared to PS (6.6 hours [4.6–9.4] vs 3.6 hours [2.9–6]; *P* = .021).

Follow-up and clinical outcomes

Median follow-up was 16 months (5–22), the minimum period was 8 days (patient with in-hospital mortality), and the maximum period was 31 months. Overall freedom from VT recurrence was 52%. When comparing patients with and without VT recurrence, intrinsic QRS width was significantly wider in those with VT recurrence compared to those without (156 ms [135–208] vs 114 ms [107–165]; $P = .024$) (Supplemental Table 2). Freedom from VT recurrence was significantly lower in patients with FS compared to PS (20% vs 80%; $P = .005$). Kaplan-Meier analysis was consistent with this difference between FS and PS ($P = .021$) (Figure 6A). Eighty-eight percent of patients with C-shaped pattern (n = 7) and 50% of patients with T-shaped pattern (n = 3) had VT recurrence. Patients with VT recurrence had significantly larger LGE volumes compared to patients without recurrence (11.4 mL [8.8–13.9] vs 4.2 mL [0–9.5]; $P = .012$) (Figure 6C). A cutpoint value of 9.6 mL of septal LGE volume demonstrated 80% sensitivity, 64% specificity, 78% positive predictive value, and 67% negative predictive value for VT recurrence (area under the curve = 0.83; $P = .002$).

Freedom from VT recurrence in patients with midmyocardial septal involvement was numerically lower than in those without (37% vs 83%; $P = .07$). All 3 patients without septal LGE remained free from VT recurrence. Two of 3 patients with lamin A/C-related cardiomyopathy had VT recurrence, of whom the 1 patient without recurrence underwent bipolar ablation after 3 previously unsuccessful ablations.

Four patients underwent heart transplantation, and 2 patients underwent LVAD implantation. Three patients with FS died during the follow-up period. One patient with FS having a C-shaped pattern underwent heart transplantation 4 days after his fifth ablation procedure, during which 9 VT morphologies were observed (Figure 7). Overall freedom from VT recurrence/LVAD/heart transplantation/death was 48% and higher in patients with PS than in those with FS (70% vs 33%; $P = .072$) (Figure 6B).

Discussion

The major findings of this study are as follows. (1) Heterogeneous septal LGE patterns and involvement were observed in patients with scar-related VT arising from anteroseptal substrate in NICM. (2) The presence of FS was powerfully predictive for recurrence after VT ablation, with a high freedom from VT observed in the absence of this pattern. (3) Distinct LGE patterns with extension into the RVOT (T-shaped pattern) and LV inferior wall (C-shaped pattern) are predictive of a wider spectrum of VT morphologies and successful termination sites.

VTs in patients with NICM have been subtyped as arising from 2 distinct anatomic regions —anteroseptal and inferolateral—with significantly higher rates of recurrence after VT ablation in the former.[3,4] We recently reported the mechanisms of periaortic VT originating from anteroseptal substrate, for which 65% of circuits showed intramural 3-dimensional circuitry.[8] The importance of recognizing and detecting septal substrate with electroanatomic mapping correlation has been well described.[2,7,11] To the best of our knowledge, this is the first quantitative analysis of the prognostic value of septal LGE patterns to predict outcomes during and after ablation.

Piers et al[6] reported that LGE mass >7.2 g in NICM patients was predictive of monomorphic VT occurrence, suggesting that substrate arrhythmogenicity can be predicted by CMR LGE volume. Despite aggressive RF ablation, 2 of 3 patients with lamin A/C-related cardiomyopathy had a VT recurrence and 1 underwent LVAD or transplant in this cohort, consistent with high reported rates of ablation failure in this population.[14]

FS exhibited a broader spectrum of VTs observed intraprocedurally compared to PS, characterized by multiple morphologies consistent with the findings of Piers et al.[3] LGE involving the midmyocardial layer was strongly associated the larger number of VT morphologies, with a trend toward a higher rate of VT recurrence.[2,5] The depth of the substrate may be an important barrier to effective ablation therapy, as well as the overall septal scar volume. Our results strongly suggest that adjunctive strategies are necessary to treat patients upfront with FS, as targeted and standard approaches seem to be ineffective for multiple morphologies. Supplemental Figure 5 shows postablation CMR in a patient with C-shaped septal LGE to assess lesion depth with incomplete transmural penetration in the anterior LV ostium. Bipolar ablation has recently been shown to be a promising therapy for such patients but was only used in 3 cases.[15] Intramural mapping with coil or chemical embolization may be useful in such cases as a primary strategy.[16,17]

T-shaped (RV extension) and C-shaped (LV extension) patterns

Bogun et al[7] reported that 10% (3/29) of NICM patients had LGE involvement of the RV. Liang et al[11] reported that 18% of LGE involved septal RV layer in NICM patients. As T-shaped patterns were associated with termination from the RV, specific patterns seen on preprocedural LGE-CMR may be useful to predict which patients require mapping and ablation from the RV side of the septum. These results extend observations from previous reports that scar assessed by CMR is associated with a critical component of the targeted ventricular arrhythmia.[7]

Prognostic value of LGE pattern

In a quantitative scar analysis by CMR, the total LV scar size was correlated with prognosis in structural heart disease.[18] Significantly different prognoses, including LVAD implantation and death, in addition to VT recurrence suggest that the CMR scar pattern may define the prognosis beyond ejection fraction in patients with anteroseptal VT, as evidenced by a large-scale study.[19] In this challenging population, knowledge of the nature of septal scar in patients presenting with anteroseptal substrate may be useful during preprocedural counseling to estimate drastically disparate ablation outcomes and the inevitable need for LVAD or transplantation. In this limited cohort, the CMR characteristics and LGE scar volume seemed to be more predictive than ejection fraction for outcomes after catheter ablation, which were not significantly different between FS and PS. In addition to septal LGE involvement, QRS width during sinus rhythm was the only significant parameter predicting VT recurrence. Betensky et al[20] reported that the presence of intraseptal scar delays transseptal conduction time during pacing, which may explain the observed association with wider QRS duration.

Consistent with previous studies, unipolar low voltage was more closely correlated with CMR than bipolar low-voltage areas due to fibrosis that was present more diffusely and at greater depth.[2,11,21] Normal CMR has been reported in patients with critical septal substrate by Liang et al.[11]

Study limitations

This study is a single-center experience with a limited number of patients, as not all patients referred for VT ablation underwent CMR. Small patient numbers in subgroups limits the conclusions from these analyses. Selection bias is present, as patients were selected based on the presence of periaortic VT morphologies rather than the presence of any septal scar on CMR, limiting generalizability. The RVOT has thinner wall thickness, and LGE may be less sensitive in detecting fibrosis. We did not quantify the entire LGE in the ventricles outside of the septum, as the primary aim of the study was to characterize the prognostic value of septal LGE. Therefore, the scar volumes with qualitative and descriptive C- and T-shaped extensions are an underestimation of overall LGE. A significant proportion of patients previously undergone ablation, and septal LGE intrinsic to the substrate may be difficult to distinguish from scar created by ablation. Genetic testing was not performed in all patients. Lastly, our ablation strategy typically targets the deceleration zone and critical diastolic or presystolic sites during VT. It is possible that extensive scar homogenization may have been more effective in patients with FS.

Conclusion

Heterogeneous patterns and extent of septal scar were revealed by LGE-CMR among patients presenting with VT arising from anteroseptal substrate. CMR may be powerfully prognostic to substratify patients with anteroseptal substrate who have greater propensities for multiple induced VT morphologies and recurrence after catheter ablation. The development of alternative upfront strategies for patients with full-length septal LGE and midmyocardial involvement may improve outcomes in this challenging population.

Supplementary Material

Refer to Web version on PubMed Central for supplementary material.

Acknowledgments

Funding source and Disclosures: Dr H. Patel was supported by NIH Grant 2T32HL007381-41A1.Dr Wang was supported by NIH Grant 5UL1TR002389-02, which funds the Institute for Translational Medicine (ITM). Dr A. Patel received funding from Philips Healthcare. All other authors have reported that they have no relationships relevant to the contents of this paper to disclose.

References

1. Yang J, Liang J, Shirai Y, et al. Outcomes of simultaneous unipolar radiofrequency catheter ablation for intramural septal ventricular tachycardia in nonischemic cardiomyopathy. Heart Rhythm 2019;16:863–870. [PubMed: 30576879]
2. Haqqani HM, Tschabrunn CM, Tzou WS, et al. Isolated septal substrate for ventricular tachycardia in nonischemic dilated cardiomyopathy: incidence, characterization, and implications. Heart Rhythm 2011;8:1169–1176. [PubMed: 21392586]

3. Piers SR, Tao Q, van Huls van Taxis CF, et al. Contrast-enhanced MRI-derived scar patterns and associated ventricular tachycardias in nonischemic cardiomyopathy: implications for the ablation strategy. Circ Arrhythm Electrophysiol 2013; 6:875–883. [PubMed: 24036134]
4. Oloriz T, Silberbauer J, Maccabelli G, et al. Catheter ablation of ventricular arrhythmia in nonischemic cardiomyopathy: anteroseptal versus inferolateral scar sub-types. Circ Arrhythm Electrophysiol 2014;7:414–423. [PubMed: 24785410]
5. Nazarian S, Bluemke DA, Lardo AC, et al. Magnetic resonance assessment of the substrate for inducible ventricular tachycardia in nonischemic cardiomyopathy. Circulation 2005;112:2821–2825. [PubMed: 16267255]
6. Piers SR, Everaerts K, van der Geest RJ, et al. Myocardial scar predicts monomorphic ventricular tachycardia but not polymorphic ventricular tachycardia or ventricular fibrillation in nonischemic dilated cardiomyopathy. Heart Rhythm 2015; 12:2106–2114. [PubMed: 26004942]
7. Bogun FM, Desjardins B, Good E, et al. Delayed-enhanced magnetic resonance imaging in nonischemic cardiomyopathy: utility for identifying the ventricular arrhythmia substrate. J Am Coll Cardiol 2009;53:1138–1145. [PubMed: 19324259]
8. Nishimura T, Beaser AD, Aziz ZA, et al. Periaortic ventricular tachycardia in structural heart disease: evidence of localized reentrant mechanisms. Heart Rhythm 2020;17:1271–1279. [PubMed: 32325198]
9. Singh A, Kawaji K, Goyal N, et al. Feasibility of cardiac magnetic resonance wideband protocol in patients with implantable cardioverter defibrillators and its utility for defining scar. Am J Cardiol 2019; 123:1329–1335. [PubMed: 30739658]
10. Marchlinski FE, Callans DJ, Gottlieb CD, Zado E. Linear ablation lesions for control of unmappable ventricular tachycardia in patients with ischemic and nonischemic cardiomyopathy. Circulation 2000;101:1288–1296. [PubMed: 10725289]
11. Liang JJ, D'Souza BA, Betensky BP, et al. Importance of the interventricular septum as part of the ventricular tachycardia substrate in nonischemic cardiomyopathy. JACC Clin Electrophysiol 2018;4:1155–1162. [PubMed: 30236388]
12. Aziz Z, Shatz D, Raiman M, et al. Targeted ablation of ventricular tachycardia guided by wavefront discontinuities during sinus rhythm: a new functional substrate mapping strategy. Circulation 2019; 140:1383–1397. [PubMed: 31533463]
13. Anderson RD, Kumar S, Parameswaran R, et al. Differentiating right- and left-sided outflow tract ventricular arrhythmias: classical ECG signatures and prediction algorithms. Circ Arrhythm Electrophysiol 2019; 12:e007392. [PubMed: 31159581]
14. Hasebe Y, Fukuda K, Nakano M, et al. Characteristics of ventricular tachycardia and long-term treatment outcome in patients with dilated cardiomyopathy complicated by lamin A/C gene mutations. J Cardiol 2019; 74:451–459. [PubMed: 31060954]
15. Della Bella P, Peretto G, Paglino G, et al. Bipolar radiofrequency ablation for ventricular tachycardias originating from the interventricular septum: safety and efficacy in a pilot cohort study. Heart Rhythm 2020; 17:2111–2118. [PubMed: 32599177]
16. Kreidieh B, Rodriguez-Manero M, Schurmann P, et al. Retrograde coronary venous ethanol:10.1161/CIRCEP.116.004352 e004352
17. Tholakanahalli VN, Bertog S, Roukoz H, Shivkumar K. Catheter ablation of ventricular tachycardia using intracoronary wire mapping and coil embolization: description of a new technique. Heart Rhythm 2013;10:292–296. [PubMed: 23089899]
18. Klem I, Weinsaft JW, Bahnson TD, et al. Assessment of myocardial scarring improves risk stratification in patients evaluated for cardiac defibrillator implantation. J Am Coll Cardiol 2012;60:408–420. [PubMed: 22835669]
19. Gulati A, Jabbour A, Ismail TF, et al. Association of fibrosis with mortality and sudden cardiac death in patients with nonischemic dilated cardiomyopathy. JAMA 2013;309:896–908. [PubMed: 23462786]
20. Betensky BP, Kapa S, Desjardins B, et al. Characterization of trans-septal activation during septal pacing: criteria for identification of intramural ventricular tachycardia substrate in nonischemic cardiomyopathy. Circ Arrhythm Electrophysiol 2013;6:1123–1130. [PubMed: 24106241]

21. Desjardins B, Yokokawa M, Good E, et al. Characteristics of intramural scar in patients with nonischemic cardiomyopathy and relation to intramural ventricular arrhythmias. Circ Arrhythm Electrophysiol 2013;6:891–897. [PubMed: 23985383]

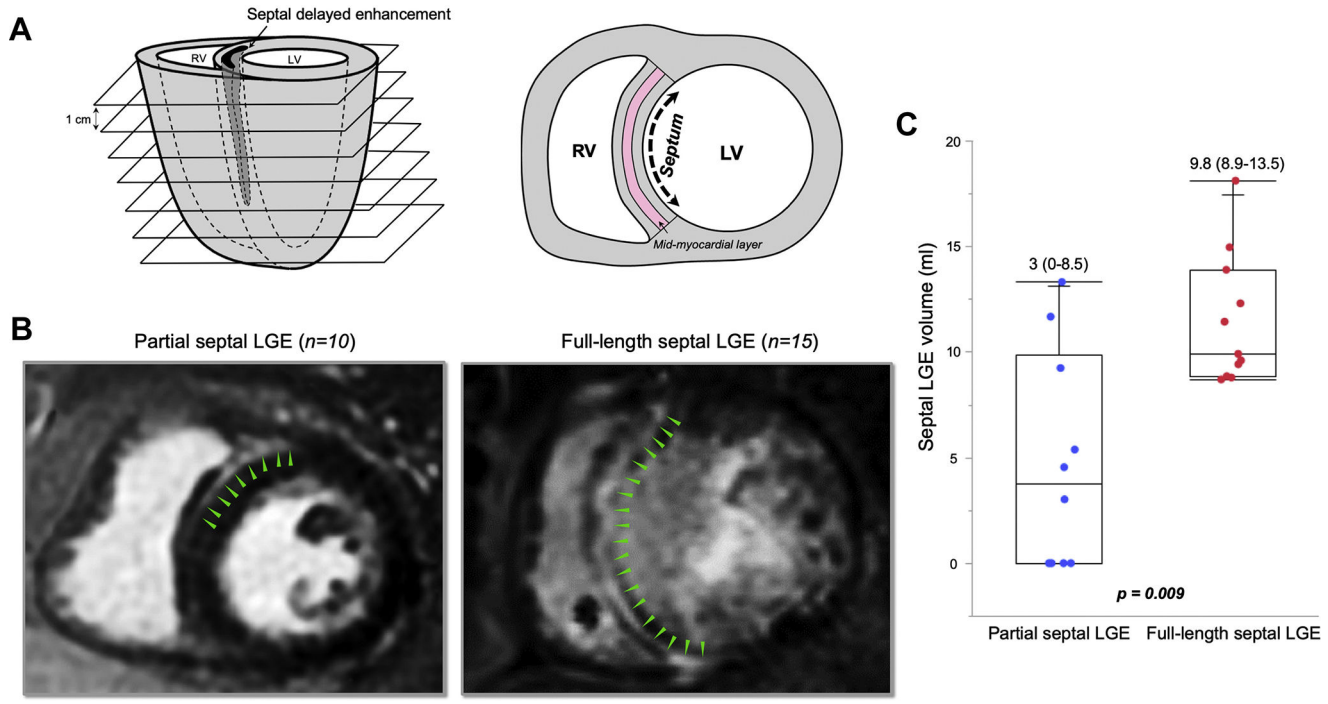

Figure 1.

Cardiac segmentation and definitions of septal extension. **A:** Analysis of late gadolinium enhancement (LGE) involvement in the short axis with 1-cm-thick slices. Interventricular septum was defined as the region between the anterior and inferoposterior right ventricular (RV) insertion points. The septal midmyocardial layer was defined as the middle third part of the septal width. **B:** Cutpoint value of longitudinal LGE involvement was ≥80% of interventricular septum between full-length septal (FS) and partial septal (PS). **Left:** Image showing 28% LGE involvement without midmyocardial layer involvement. **Right:** Image showing 100% involvement within interventricular septum. **C:** Septal LGE volume was significantly larger in patients with FS than in those with PS. LV = left ventricle.

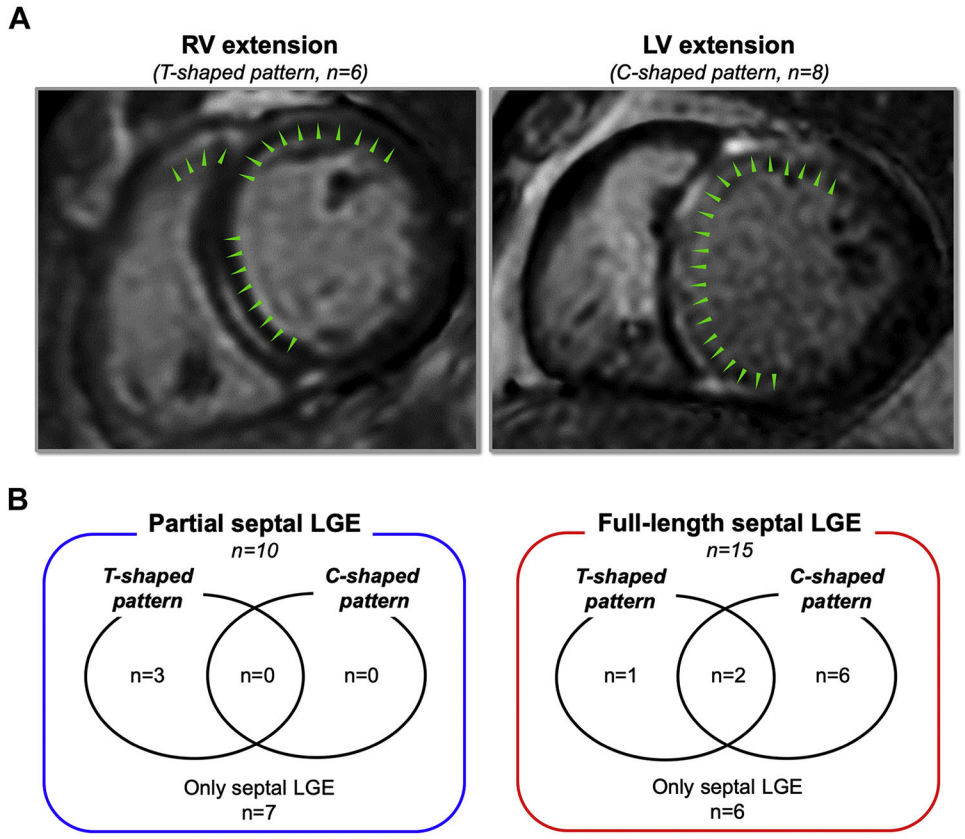

Figure 2.

Two morphologic patterns of concomitant LGE with anteroseptal LGE. **A:** RV extension (T-shaped pattern) was defined LGE in the RV outflow tract. LV extension (C-shaped pattern) was defined LGE continuously extending from septal region to LV anterior and/or inferior lateral wall. **B:** Twenty-percent (n = 3) of FS patients and 30% (n = 3) of PS patients had a T-shaped pattern. C-shaped pattern was observed in 32% of patients (n = 8), all having FS. Abbreviations as in Figure 1.

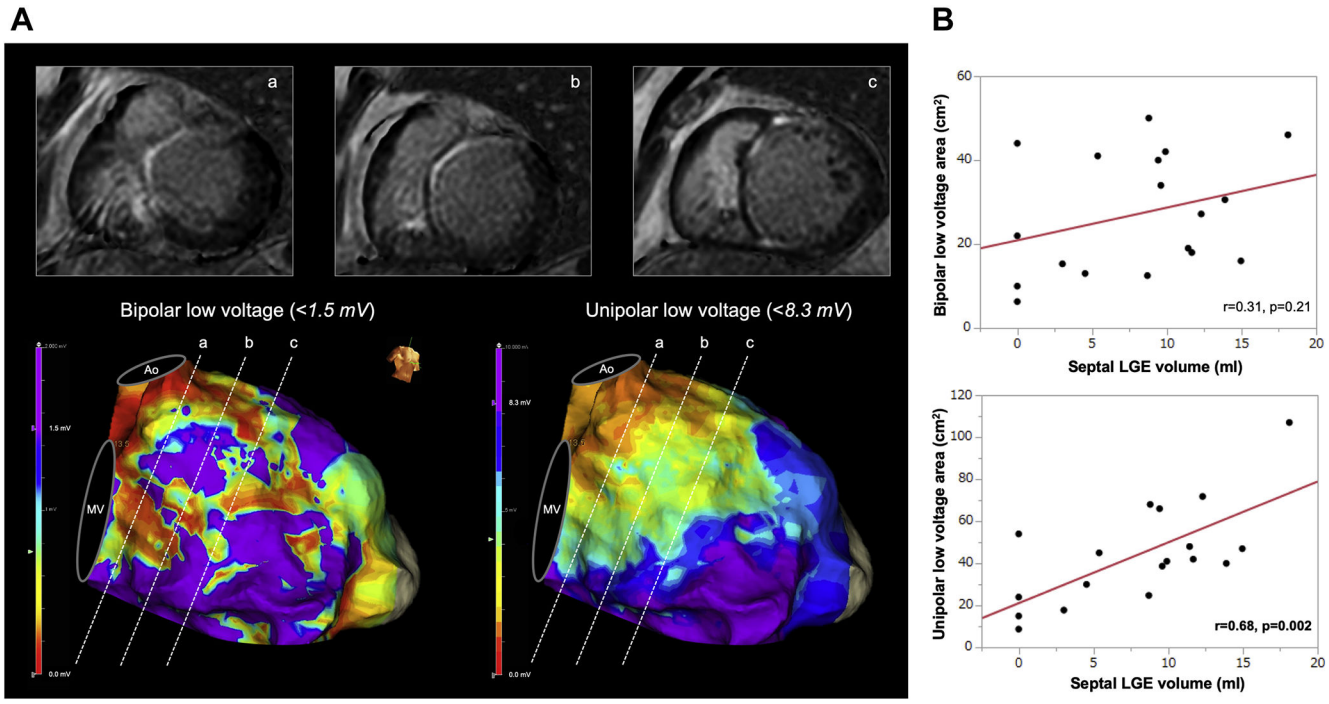

Figure 3.

Correlation between LGE volume and low-voltage area. **A:** Patient with FS. Three basal cardiac magnetic resonance imaging slices. In the bipolar voltage map, heterogeneous low voltage is seen, whereas the majority of the septum shows abnormal unipolar low voltage, concordant with septal LGE. **B:** Unipolar low-voltage areas correlated with LGE volume, whereas bipolar low-voltage areas did not. Ao = aorta, MV = mitral valve, LGE = late gadolinium enhancement

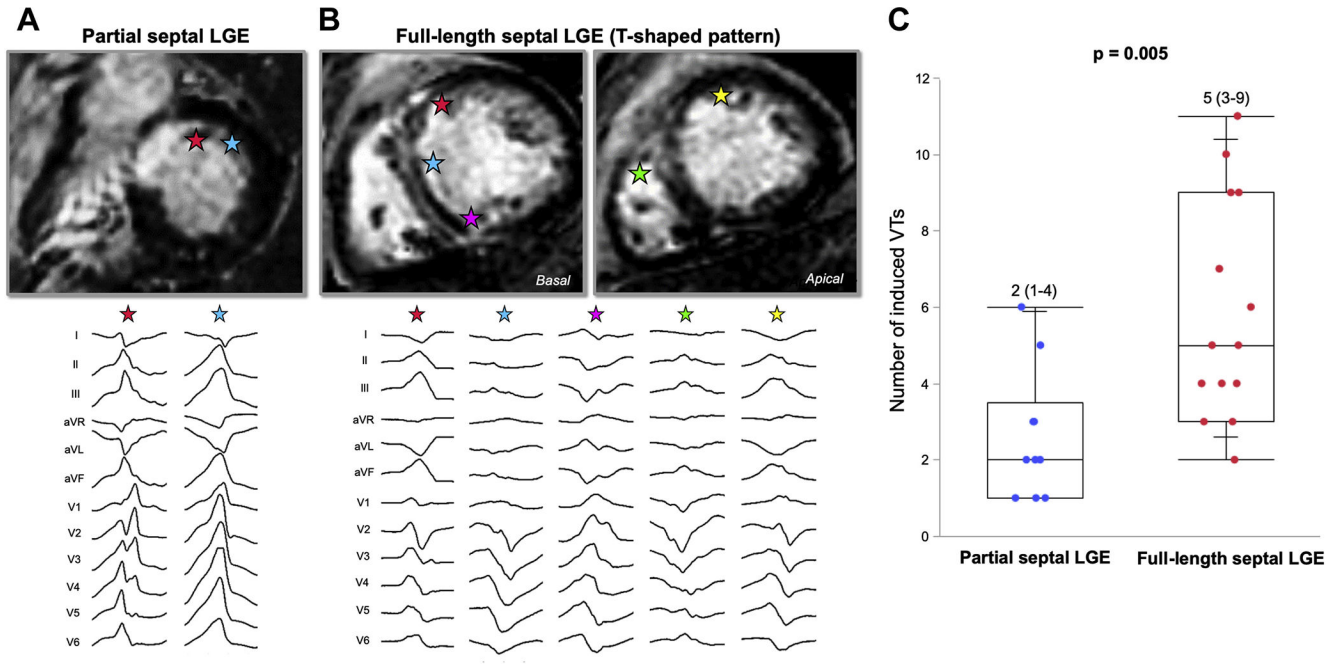

Figure 4.

Spectrum of ventricular tachycardia (VT) morphologies observed in patients with FS vs PS LGE. **A:** PS patient with C-shaped pattern had 2 VT morphologies. *Stars* indicate exit sites of VTs. **B:** FS patient with T-shaped pattern had 5 VTs with various morphologies. **C:** Number of VT morphologies was greater in patients with FS than in those with PS. Abbreviations as in Figure 1.

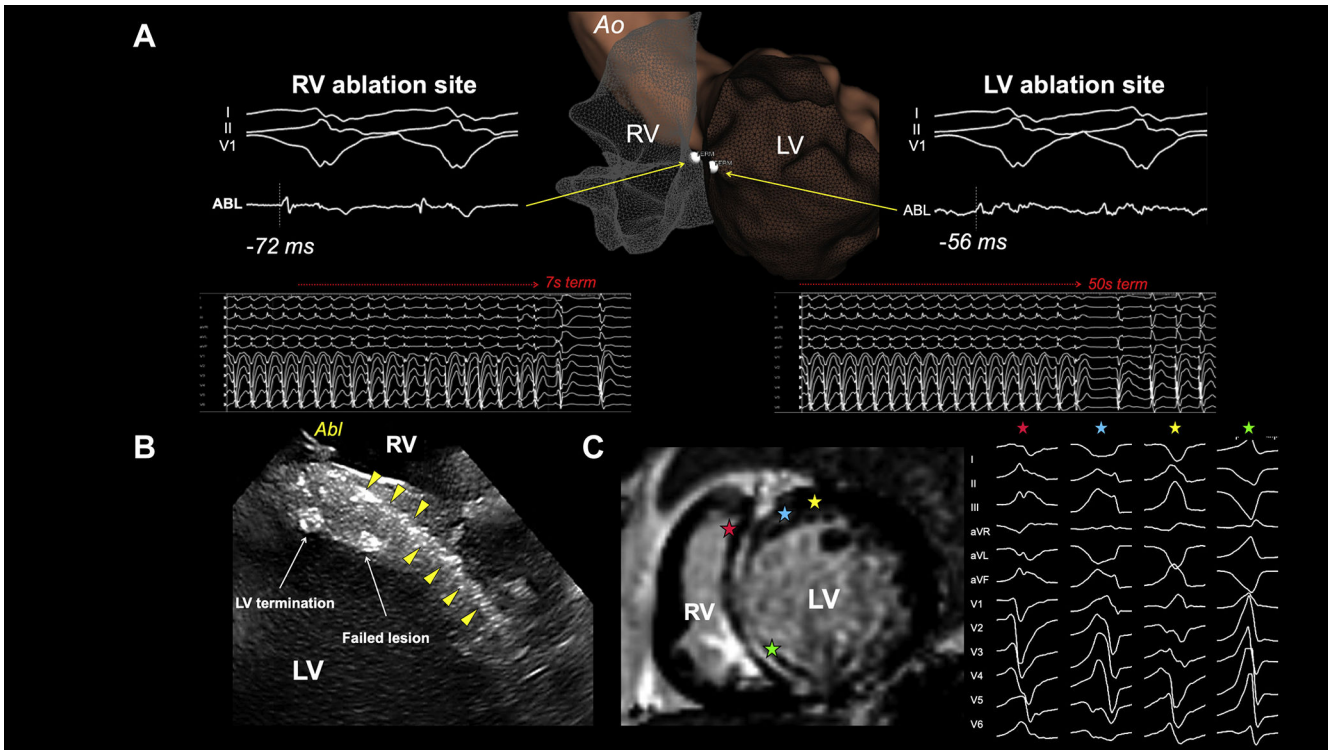

Figure 5.

VT termination from both sides of the ventricular septum in a patient with FS LGE. **A:** Faster termination was achieved during ablation from RV with presystolic potential (−72 ms) compared to LV with −56 ms presystolic potential. **B:** Intracardiac echocardiography showed a septal stripe *(yellow triangles)* and successful VT termination sites from both ventricles. **C:** Cardiac magnetic resonance image with FS and induced VT. *Stars* indicate exit sites of VTs. Abbreviations as in in Figures 1

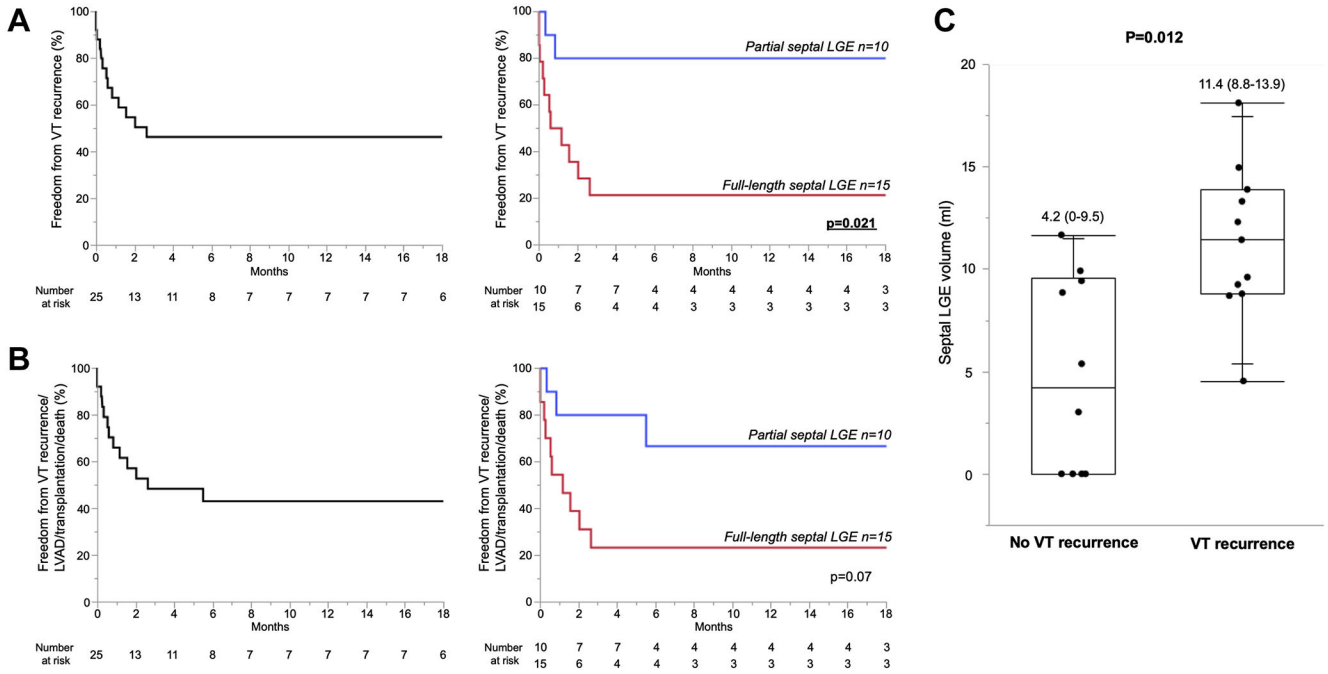

Figure 6.

Follow-up outcome after ablation procedure. **A:** Freedom from VT recurrence was 52% and significantly higher in patients with PS compared to patients with FS (82% vs 21%; *P* = .003). **B:** VT recurrence/left ventricular assist device (LVAD)/heart transplantation/death-free survival probability was 48% and higher in patients with PS compared to patients with FS (73% vs 29%; *P* = .028). **C:** Patients with VT recurrence had significantly larger LGE volume compared to patients free from recurrence. Abbreviations as in Figures 1

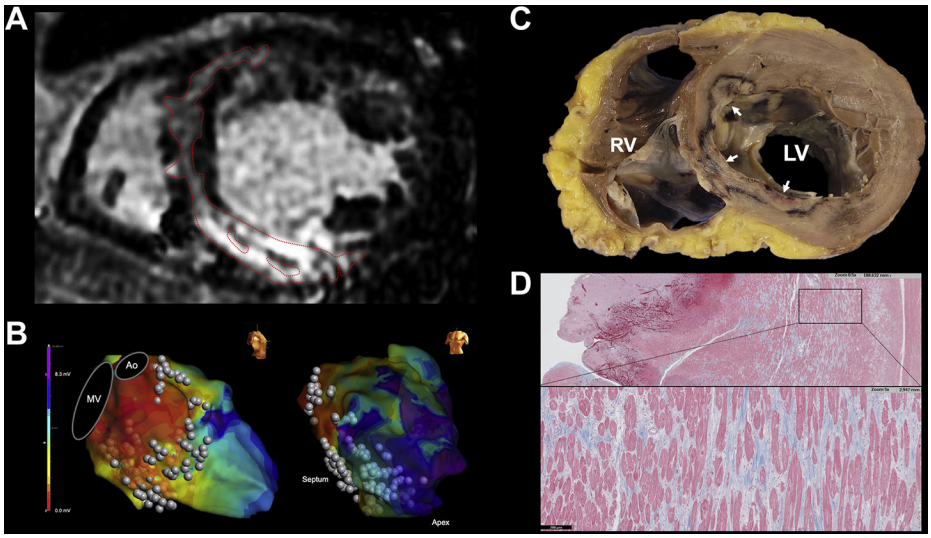

Figure 7.

Pathologic analysis of septal scar and ablation lesion. **A:** FS patient with C-shaped pattern underwent heart transplantation 4 days after a fourth unsuccessful ablation procedure. **B:** Ablation along the entire septum and LV inferior wall with low unipolar voltages shown on electroanatomic mapping. **C:** Explanted heart showed incomplete penetration of multiple ablation lesions into the midseptum *(white arrows)*. **D:** Trichrome stain showing extensive midseptal fibrosis with interspersed viable myocardium. Ao = aorta; MV = mitral valve; other abbreviation as in Figure 1.

Table 1

Baseline characteristics

	Total patients (N = 25)	Partial septal LGE (n = 10)	Full-length septal LGE (n = 15)	*P* value
Age (yr)	64 ± 8	66 ± 7	63 ± 9	.38
Male	23 (92)	9 (90)	15 (100)	.21
LVEF (%)	39 (24–47)	43 (35–51)	30 (22–45)	.19
Intrinsic QRS width (ms)	133 (113–188)	114 (108–133)	156(123–210)	.071
Coronary artery disease	4(16)	3(30)	1(7)	.27
Hypertension	10 (40)	4 (40)	6(40)	1
Diabetes mellitus	7(28)	3(30)	4(27)	1
Atrial fibrillation	11 (44)	3(30)	8(53)	.41
Cardiac device				
ICD	14 (56)	7(70)	7(47)	.41
CRT-D	10 (40)	2 (20)	8(53)	.21
VT storm	8(32)	2 (20)	6(40)	.4
Amiodarone use	20 (80)	6 (60)	14 (93)	.12
Other antiarrhythmics use	12 (48)	4 (40)	8(53)	.69
Beta-blocker use	23 (92)	9 (90)	14 (93)	1
Aortic valve surgery	2(8)	0(0)	2(14)	.5
Previous VT ablation	12 (48)	4 (40)	8(53)	.69
3	3(12)	1(10)	2(13)	
2	3(12)	1(10)	2(13)	
1	6(24)	2 (20)	4(27)	
0	13 (52)	6 (60)	7(47)	
Clinical VT				
Right bundle branch block	12 (48)	4(40)	8(53)	.69
Inferior axis	18 (72)	7(70)	11 (73)	1
Left axis	12 (48)	6 (60)	6(40)	.43
Epicardial access	9(36)	3(30)	6(40)	.69

Values are given as n (%), mean ± SD, or median (interquartile range) unless otherwise indicated.

CRT-D = cardiac resynchronization therapy–defibrillator; ICD = implantable cardioverter-defibrillator; LGE = late gadolinium enhancement; LVEF = left ventricular ejection fraction; VT = ventricular tachycardia.